ISSN 1075-7015, Geology of Ore Deposits, 2023, Vol. 65, No. 4, pp. 315–331. © Pleiades Publishing, Ltd., 2023.
Russian Text © The Author(s), 2023, published in Geologiya Rudnykh Mestorozhdenii, 2023, Vol. 65, No. 4, pp. 337–353.

The Sb–As Lojane Deposit (Republic of North Macedonia): Types of Ores and Conditions of Their Occurrence and Geochemical Features

T. Serafimovskii[a], A. V. Volkov[b, *], T. Đorđevic[c], G. Tasev[a], D. Serafimovskii[a], K. Yu. Murashov[b], and L. Georgiev[a]

[a] *Goce Delčev University, Štip, North Macedonia*
[b] *Institute of Geology of Ore Deposits, Petrography, Mineralogy, and Geochemistry, Russian Academy of Sciences, Moscow, 119017 Russia*
[c] *Department of Mineralogy and Crystallography, University of Vienna, Vienna, 1090 Austria*
**e-mail: tma2105@mail.ru*

Received July 15, 2022; revised November 21, 2022; accepted February 20, 2023

Abstract—This article presents the results of comprehensive studies of Sb–As ores from the Lojane deposit, located in the northeastern part of the Republic of North Macedonia, near the border with Serbia. Five types of Sb–As ores are distinguished in the deposit: brecciated realgar orpiment ores; realgar breccias; brecciated antimonite ores; massive, almost monomineral realgar ores; and realgar–antimonite nested ores. The ores are characterized not only by the unusual paragenesis of minerals of nickel, arsenic, and antimony, but also by a very close fusion of antimonite, realgar, and collomorphic quartz. A wide range of elements in ores (As, Sb, Cr, Ti, Mn, Ni, Mo, Co, Ag, Tl, U, etc.) is likely due to the combination of mineralization from multiple distinct parageneses that occurred at different times. Thermometric studies of fluid inclusions in quartz indicate a temperature range of T_{hom} varying from 180 to 220°C, with an average value of 201°C. Studies of the isotopic composition of sulfur in antimonite and realgar showed fairly narrow intervals of $\delta^{34}S$ values from –5.19 to –0.26‰ and from –4.80 to 1.92, respectively, indicating an endogenous sulfur source. Based on these findings, the Lojane deposit can be attributed to the epithermal class.

Keywords: Republic of North Macedonia, Vardar zone, Lojane deposit, serpentinites, antimony, arsenic, ore textures, geochemistry, fluid inclusions, sulfur isotopic

DOI: 10.1134/S1075701523040050

INTRODUCTION

The Lojane field is located in the northeast of the Republic of North Macedonia (RNM), a few kilometers from the border with the Republic of Serbia, about 10 km northwest of the city of Kumanovo and 40 km north of the city of Skopje (Fig. 1). Ore cores containing Sb and As, along with Ni, Co, and U, were discovered during the development of the chromium deposit. The Lojane deposit is small in terms of chromium reserves and medium in terms of antimony reserves. About 300 thousand t of chromium ore with an average content of 30% CR_2O_3 (Schumacher, 1954) and about the same amount of Sb–As ore with a content of 2.5–4% Sb and 5–7.3% As were extracted within it. Annual production rate ranged from 11000 to 15000 t of ore (Antonovic, 1965).

The Lojane mine operated from 1923 to 1979. At the first stage (until 1953), chromite-containing, silicified serpentinite (Schumacher, 1954) was extracted, and Sb–As veins were mined starting from 1954. Geological studies of the Lojane deposit began in the first half of the 20th century (Hiessleitner, 1931, 1934, 1951; Schumacher, 1954) and were mainly focused on chrome ores. Later, the attention of the researchers was attracted by Sb–As vein mineralization (Jankovic, 1960; Radusinovic, 1966). A number of later papers have focused on platinum group minerals found in chromite ore (Grafenauer, 1977; Augé et al., 2017). The results of geochemical studies on the field area are presented in the article (Mudrinic, 1978). The results of metallogenic research in the Lojane field are given in the monograph (Serafimovski, 1993). A number of recent publications (Alderton et al., 2014; Tasev et al., 2017; Djordjevic et al., 2019; et al.) address environmental aspects.

In this article, we have updated the geological characteristics of the area and the Lojane deposit itself. For the first time, the results are presented and discussed of studying the geochemical features of Sb–As ores. Conclusions about the conditions of formation of Sb–As mineralization are made on the basis of studies of

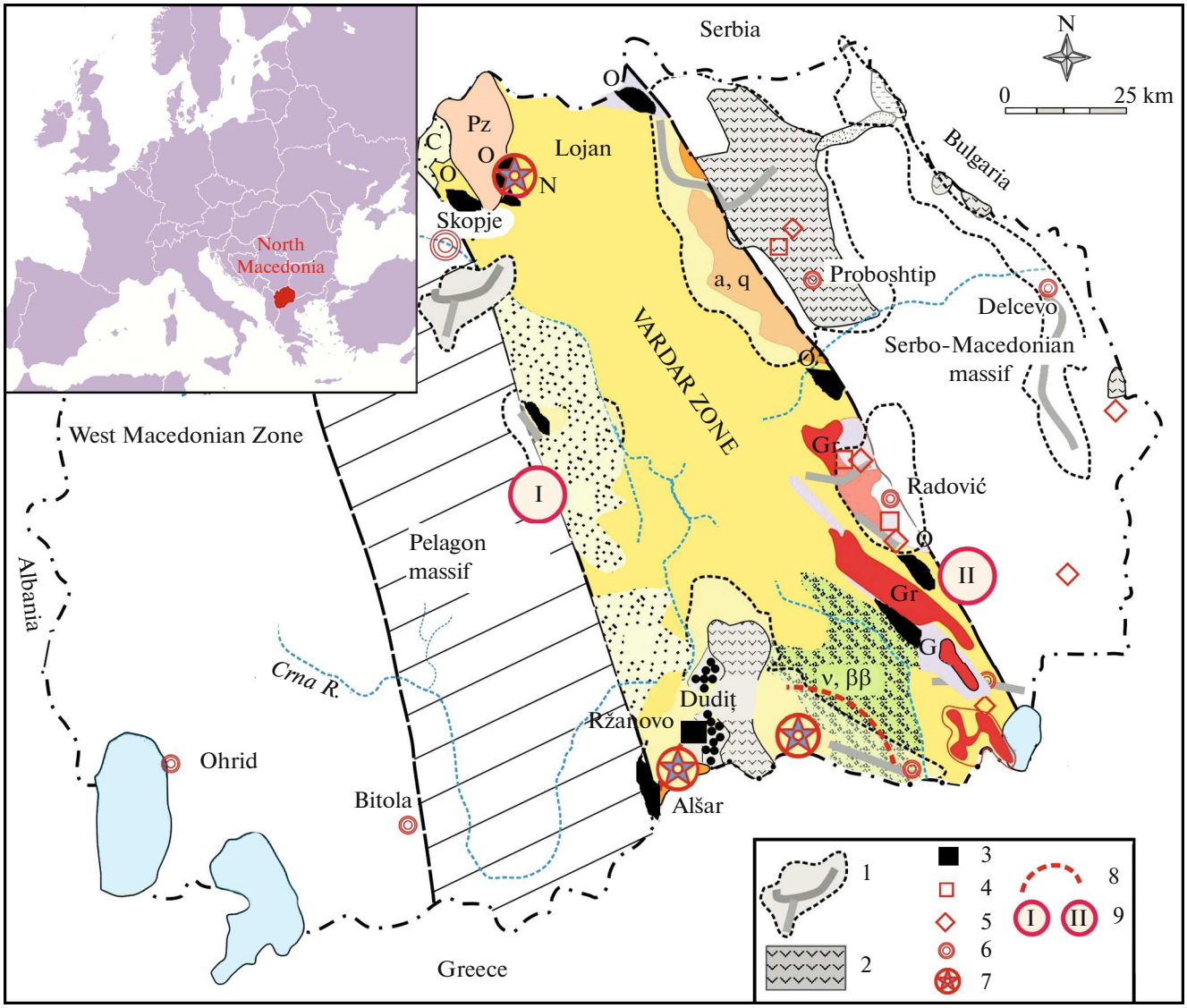

Fig. 1. Position of the Lojane field in the Vardar zone. A map from the article (Boev, Jankovic, 1996) was used. (1) Potential ore areas, (2) Tertiary volcanic rocks, (3) Fe–Ni–Cr deposit, (4) Cu–Au deposit, (5) Cu deposit, (6) town, (7) promising ore deposits, (8) Kozuf volcanic zone, and (9) regional lineaments. *Abbreviations:* N—Neogene and Paleogene sedimentary strata; a, q—volcanoes (tertiary); C—Cretaceous sedimentary strata; Gr—granitoids (Jurassic); Pz—Paleozoic metamorphic rocks; G—gneiss (Precambrian); Jurassic ophiolites: ν, ββ—Gabbro-diabase, O—dunites and/or harzburgites, P—pillow lava and associated sediments.

fluid inclusions in gangue quartz. To assess the sources of ore, the isotopic composition of the sulfur of the main sulfide minerals was studied.

MATERIALS AND METHODS

A collection of representative samples of Sb–As ores from the Lojane deposit was obtained from surface exposures, core samples from drilling wells, and exploration trenches. Numerous thin sections were prepared from the samples and examined under a polarizing optical microscope Zeiss Axiolab Pol in reflected light mode (magnification ranging from 50× to 640×).

A batch of 12 samples intended for ICP-AES analysis was processed following the international standard ISO 14869-1:2001. Sample analysis for 33 elements was conducted using an Inductively Coupled Plasma Atomic Emission Spectrometer (Varian 715-ES) in the analytical laboratory of Goce Delčev University in Stip, Republic of North Macedonia. The samples from ore concentrates, flotation tailings, and ore-hosting serpentinites were analyzed by ICP-MS for 59 elements, on an ICP-ES/MS instrument

(AQ200) at the Bureau Veritas Minerals (BVM) Laboratory (Vancouver, British Columbia, Canada).

Detailed microthermometric studies of fluidic inclusions in double-sided polished plates of gangue quartz were carried out at the Department of Mineralogy, Petrology, and Economic Geology of the University of Aristotle (Thessaloniki, Greece) using a measuring complex consisting of a THOMM-600/TMS 90 LINKAM camera (United Kingdom), connected with a Leitz lux-POL microscope, under the guidance of Prof. Dr. Vasilios Melfos.

To obtain $\delta^{34}S$ values, monomineral antimonite and realgar samples were ground to 200 mesh using an agate mortar. Sulfur isotope analysis was performed at the ACME laboratory of the Department of Geological Sciences, Queen's University of Kingston, Ontario, Canada. The results are presented as $\delta^{34}S$ values, which were calculated by normalization of the ratios of $^{34}S/^{32}S$ in samples to that of the Vienna Canyon Diablo Troilite (V-CDT) international standard. $\delta^{34}S$ values are in units (‰) and are reproducible up to ±0.2‰.

FEATURES OF THE GEOLOGICAL STRUCTURE OF THE DEPOSIT

The ophiolitic complex of rocks containing the Lojane deposit is located in the eastern part of the Vardar zone on the border with the Serbian–Macedonian massif (Fig. 1) and is traced along a stretch of 11 km with a width of 1–4 km. The complex is presented in three series: (1) the main mantle series, in which harzburgite dominates, dunite is present in smaller volumes, and intermittent bodies and veins of pyroxenite are noted in places, overlain by rocks of (2) a cumulative series, including dunite, followed by lherzolite, pyroxenite, and gabbro, and (3) the uppermost volcanosedimentary series. A distinctive feature of this complex is that it is intruded by numerous small tertiary bodies of granitoids and dacite andesites.

In the area of the Lojane deposit, the ultrabasic rocks of the Jurassic ophiolitic complex of the Vardar zone are strongly metamorphosed and are represented by serpentine and silicified serpentinites (Fig. 2). The geological structure of the area also includes Jurassic limestones, Upper Cretaceous flysch, Tertiary rhyolites, and black tufa clays, as well as Neogene clay deposits.

The chromite mineralization of the Lojane deposit in the form of small pencil-shaped bodies is hosted by serpentinites formed by rocks of the harzburgite series. Sb–As mineralization is mainly hosted by silicified serpentinites at the contact with rhyolites; in addition, it is locally developed in chromite deposits. Antimonite–realgar veins extend (more than 400 m) along the contact between the lenticular body of rhyolite and serpentinite and partially continue in serpentinite (Figs. 2, 3).

In addition, small deposits are known of antimonite with traces of realgar immediately in two lenses of silicified serpentinite at a distance of 100 and 400 m from the contact with rhyolites (Figs. 2, 3).

MORPHOLOGICAL FEATURES OF Sb–As ORE BODIES

The morphological features of Sb–As ore bodies of the Lojane deposit are caused by lithological features and tectonic development of the host rocks. Complex vein bodies are formed at the contact of rhyolite and serpentinite (Figs. 4b, 4c), while they are more simple in serpentinite (Fig. 4a). A certain morphological similarity of ore formations with featherlike fractures is observed in adits 14 and 22/1 at 480 m (Fig. 4b). In the Sb–As rhyolites, the mineralization forms a stockwork of centimeter-long veins that are roughly orthogonal to each other (Fig. 4c).

At a distance from the contact of rhyolite and serpentinite Sb–As veins are ruptured and deformed (Figs. 4b, 4c). The Sb–As mineralization here is represented by a series of veins and fracture deposits. In some places, the veins bend and change their strike direction (adits 3, 4, and 6 at 480 m). Such bends are associated with the veins crossing the zone of a large meridional fault. Not far from this fault zone are the "roots" of the main ore bodies of the deposit. Further to the northwest, within the silicified bodies in serpentinites (Figs. 2–4), three separate Sb–As veins are known that are simple in structure, partially deformed, and with a steep dip angle.

ORE TEXTURES

Most of the Sb–As ores at the Lojane deposit are mineralized silicified breccias (Figs. 5a, 5b), which are typical both for the crushing zone at the contact between rhyolites and serpentinites and for rhyolites themselves, which also underwent cataclasis and silicification. In some places, disseminated antimonite and pyrite mineralization is observed in the breccia cement.

An illustrative example is typical antimonite breccias with silica cement (adit 16), as well as antimonite breccias with nickel-containing pyrite in the cement (Figs. 5a, 5b). Predominantly realgar breccias are found in the 453-m horizon (adit 19) below the realgar–antimonite vein, a manifestation of peculiar zoning (Figs. 5c, 5d). Additionally, poor antimonite mineralization is known in siliceous breccias of the Lojane deposit (Fig. 5h).

The massive ores of the Lojane deposit are composed of realgar, realgar–orpiment, and sometimes earthy realgar (Figs. 5d, 5e). In some areas, these ores are intersected by later cross-cutting antimonite veinlets of the second/third generation, which is characteristic of fault zones where realgar bodies undergo cataclastic deformation, become mineralized by later-

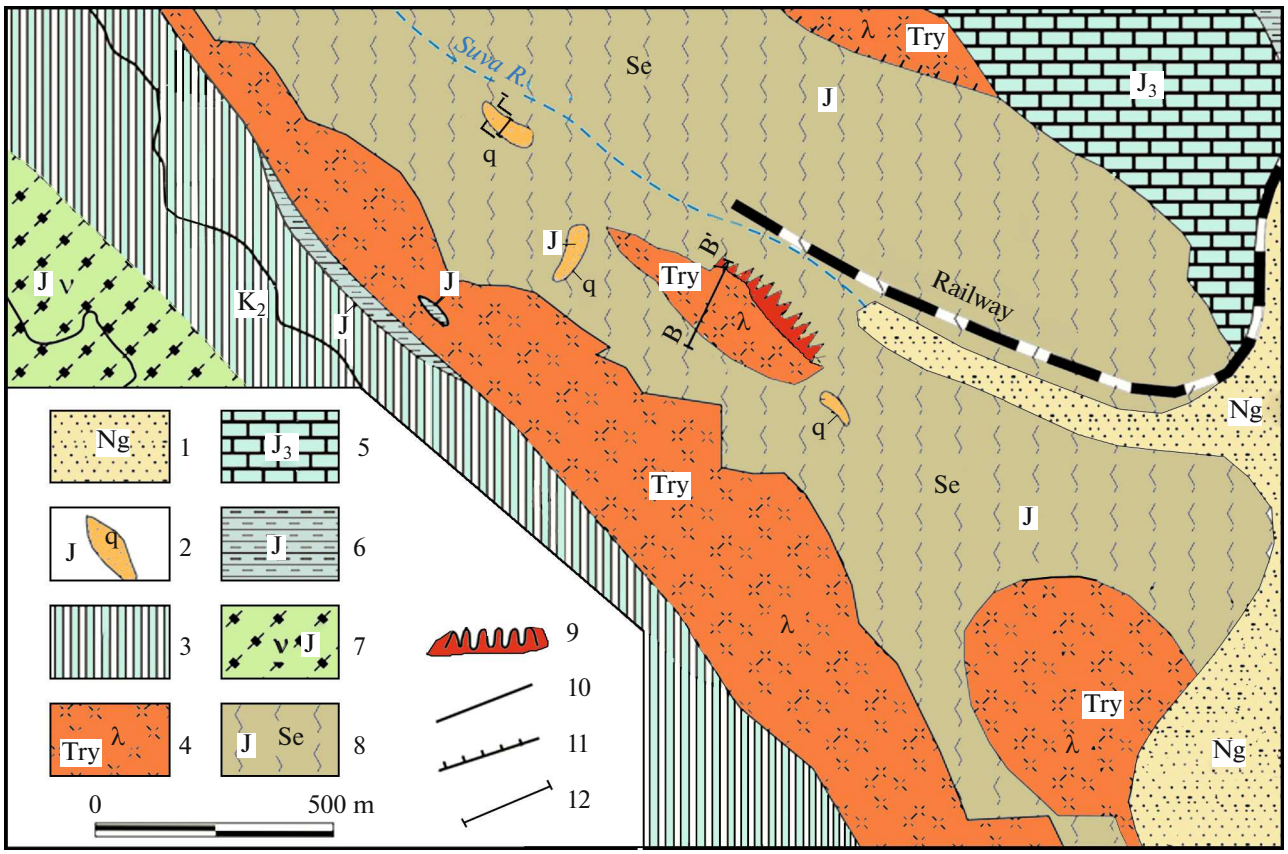

Fig. 2. Geological map of the Lojane deposit area, based on (Tasev et al., 2018) and modified. (1) Alluvial modern and Neogene clay deposits (Ng); (2) Jurassic (J) silicified serpentinites; (3) Upper Cretaceous (K_2) flysch; (4) Tertiary (Try) rhyolites; (5) Upper Jurassic (J_3) massive limestone; (6) Jurassic (J) black shales and sandstones; (7) Jurassic gabbro, diorites; (8) Jurassic (J) serpentinites and peridotites; (9) Sb–As mineralization at the contact of serpentinites and rhyolites; (10) thrust faults; (11) thrusts; and (12) lines of geological cross sections.

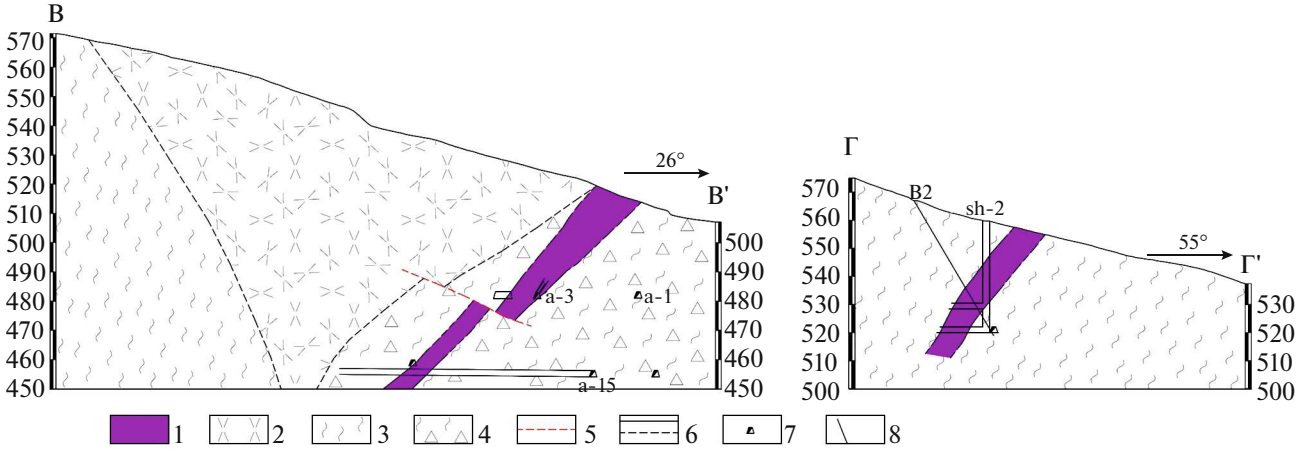

Fig. 3. Geological cross sections across the extension of Sb–As ore bodies of the Lojane deposit. Refer to Fig. 2 for the lines of the cross sections. (1) Sb–As ore body, (2) rhyolites, (3) serpentinites and peridotites, (4) brecciated serpentinites, (5) fault, (6) geological boundaries, (7) adits, and (8) borehole; sh—mine shaft.

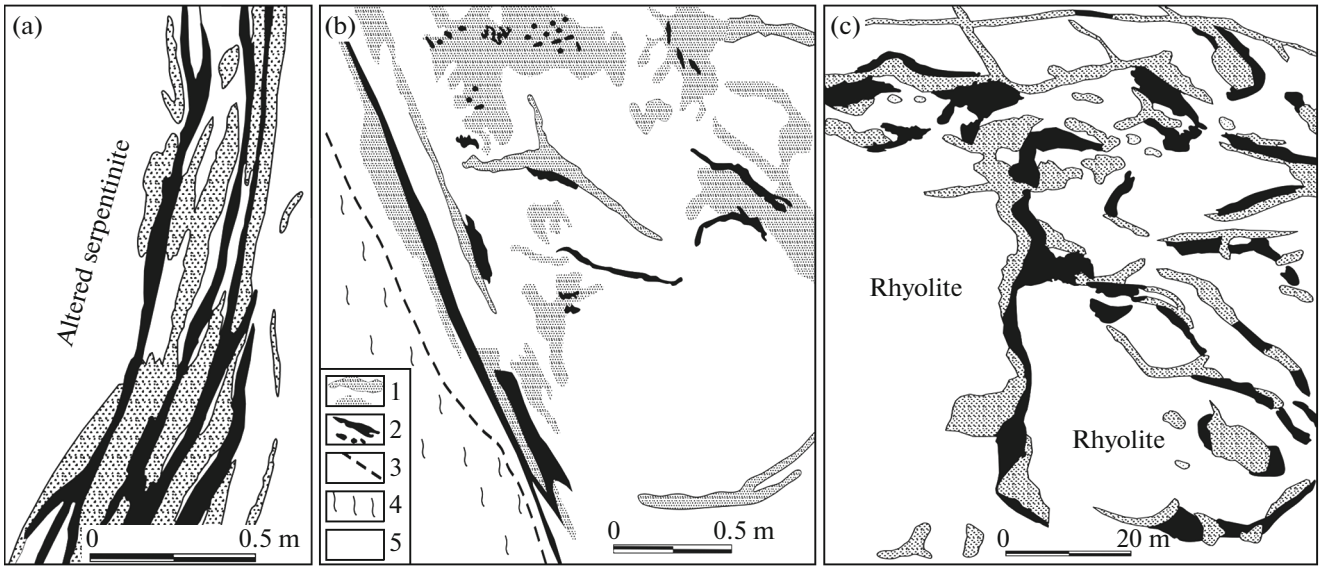

Fig. 4. Morphological features of Sb–As mineralization at the Lojane deposit (in plan view): (a) realgar–antimonite vein in altered serpentinite, Lojane deposit, horizon 461 m; (b) "feathery" distribution of Sb–As mineralization at the contact between rhyolite and serpentinite; and (c) mineralization in rhyolite, 51 m away from the contact with serpentinite. (1) Realgar, (2) antimonite, (3) border of body of serpentinites, (4) serpentinite, and (5) rhyolite.

stage antimonite, and are silicified. The most characteristic ores for the Lojane deposit are vein-type ores (Fig. 5e), which are often silicified and resemble nest-like lenses composed predominantly of antimonite (Fig. 5j).

MINERAL COMPOSITION OF ORES

Sb–As mineralization of the Lojane deposit has been studied since the beginning of the 20th century (Hiessleitner, 1931, 1934, 1951; Schumacher, 1954; Antonović, 1955, 1965; Deleon, 1959). Data on the mineral composition of ores can be found in works (Antonovic, 1965; Mudrinic, 1978; Serafimovski, 1990; etc.). A fairly detailed account of the composition of Lojane ores was published in recent works (Auge et al., 2017; Kolitsch et al., 2018; Djordjevic et al., 2018). Therefore, in this section, we limited ourselves to a brief generalization and photos of typical ore minerals (Fig. 6).

In total, 45 minerals were identified at the Lojane deposit, some of which are related to rock-forming (clinochlor, spinel, uvarovite, etc.), and the other to accessory minerals (zircon, monacite, brusitis, rutile, etc.); there are secondary minerals (romeite, annabergitis, comfinitis, limonite, gypsum, gercinite, kaolinite, etc.). The main ore minerals include Realgar and antimonite, in association with which galenite, pyrite, chalcopyrite, arsenopyrite, mauherite, scorodite, etc., are found in ores. The mineralization sequence diagram is shown in Fig. 7.

GEOCHEMICAL FEATURES OF ORES

The results of the analysis of trace elements in ores, ore concentrates, and tails of the enrichment of the Lojane deposit are presented in Tables 1 and 2 and Fig. 8, in which they are normalized to mean values for the upper crust and upper mantle (Taylor and McLennan, 1988). From Table 1, it can be seen that the majority of ore samples taken from outcrops, exploration rods and drilling wells of the field show high concentrations of As, SB, CR, and Ni and increased concentrations of Mn, TI, Tl, Mo, Zn, V, and U. As is shown in Fig. 8, ores are characterized by enrichment with a wide range of elements, compared to the average values for the upper crust (Taylor and McLennan, 1988).

The enrichment factors vary from several (Bi, Co, Cd, Ag, W, Cu, Pb, Zn, Tl, and U) to dozens (Cr, Ni, Se, Mo, and Re), hundreds (As), and thousands (Sb) of times (Table 1, Figs. 8d, 8e), which probably indicates the geochemical affinity of a number of trace elements and their synchronous participation in ore formation. Such a wide range of enrichment of elements may is due to the combination in the ores of mineralization of several different time paragenesis (see above). It is noteworthy that enrichment ratios in ore concentrates (Table 2, Fig. 8b) do not exceed those in ore samples and even below them. At the same time, the enrichment ratios in the tailings (Fig. 8a) are comparable with those in ore samples (Fig. 8e) and concentrates (Fig. 8b), which indicates high losses (about 50%) of the useful components during enrichment. The spectrum of microelement enrichment in the sur-

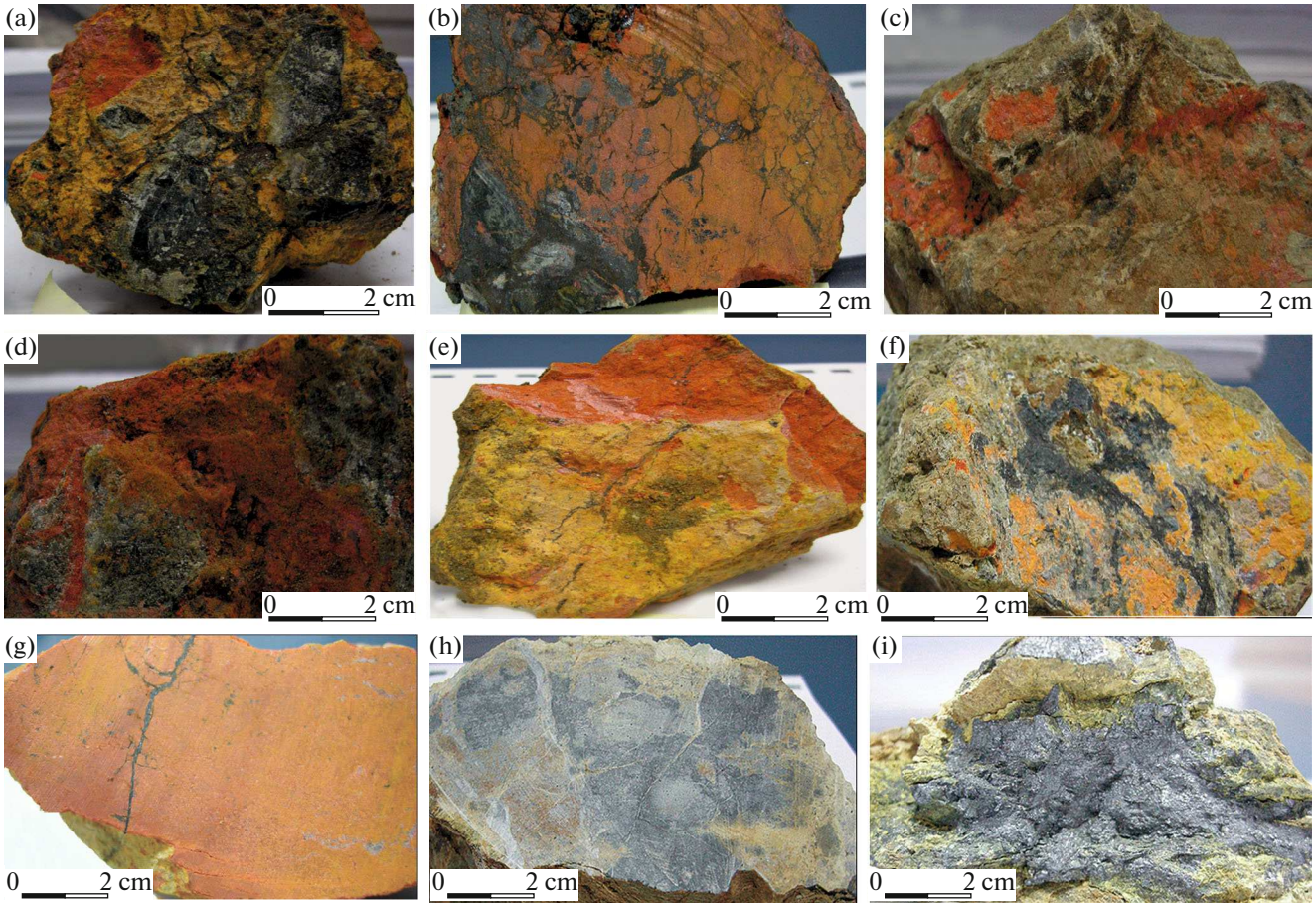

Fig. 5. Textures of Sb–As ores from the Lojane deposit: (a) brecciated realgar–orpiment ores in the serpentinite crushing zone, (b) brecciated realgar ores with antimonite matrix, (c) realgar mineralization in brecciated and silicified serpentinite, (d) conglomerate-like silicified rhyolites mineralized by late realgar, (e) typical earthy massive realgar mineralization, (f) massive realgar–orpiment mineralization in altered rhyolites intersected by late antimonite veins, (g) antimonite mineralization in silicified breccia, (h) typical realgar–antimonite mineralization in silicified nested-lens-shaped ore veins, and (i) lenticular-nested primary antimonite mineralization in silicified rhyolites.

rounding host rocks (Fig. 8c) is equally wide as that of the ores, tailings, and concentrates (Figs. 8a, 8b, 8e). However, the enrichment coefficients in the host rocks are lower by an order of magnitude or more.

The composition of the REE of ore concentrates, flotation tails, and host rocks of the Lojane deposit is given in Table 2, and the REE spectra normalized to chondrite are shown in Fig. 7e. An abnormally low content of ΣREE (from 3.3 to 10.9 g/t) is characteristic of ore concentrates of the Lojane deposit. A reduced content of ΣREE (from 27.36 to 80.55 g/t) is seen for flotation tails, and the highest content (111.03) is noted in serpentinites (see table 2).

Therefore, the data of Table 2 and Fig. 8f show that, in the studied ores and the serpentenites containing them, light REE predominate. REE serpentinites normalized to chondrite form a slightly inclined twin-chondrite spectrum with a small europium minimum (see Fig. 8f).

FLUID INCLUSION RESULTS

Fluid inclusions suitable for microthermometric studies were found in only three samples of quartz (Fig. 9) from the epithermal veins of the Lojane deposit. Sample LOJ/1 is selected from a striped core consisting of a collomorphic microgranular and coarse-grained quartz in alternating bands containing realgar (Fig. 9a). Samples LOJ/2 and LOJ/3 were made of pale green quartz (Figs. 9b, 9c).

The samples contain a limited number of very small fluid inclusions (<9 μm). Therefore, only thermometry yielded results (15 inclusions were studied) and cryometry could not be done. The microgranular quartz from sample LOJ/1 is completely free of fluid inclusions (Fig. 9a).

Several inclusions were found in the strips of coarse-grained quartz (Fig. 10b). The inclusions are either very small in size or show changes after capture and are empty (Figs. 10 c, 10d, 10i). Samples LOJ/2

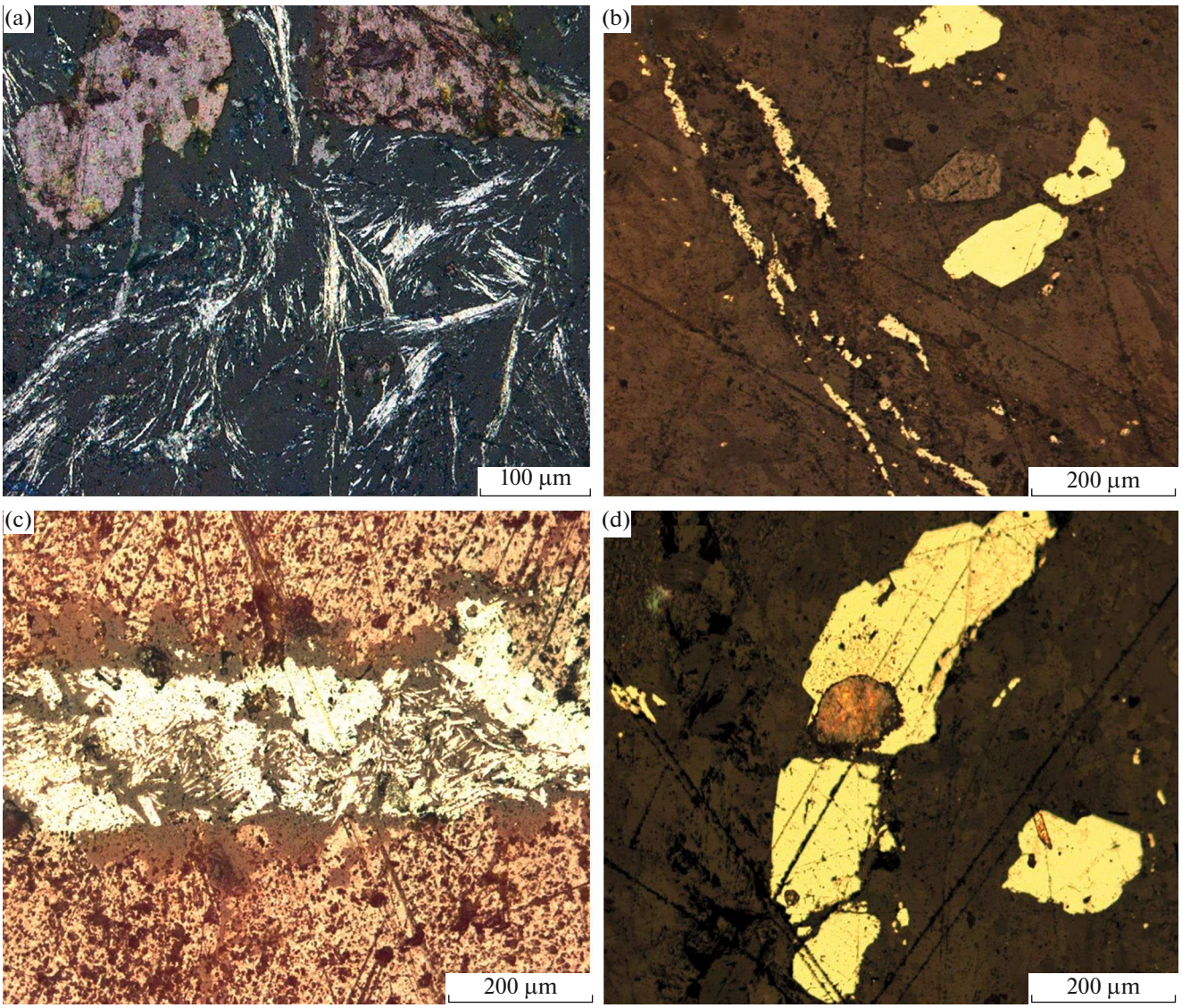

Fig. 6. Main minerals of ores of the Lojane deposit, (a) sheetlike relic aggregates of thin-prismatic antimonite with a characteristic horsetail structure in realgar, (b) typical discontinuous veins of antimonite adjacent to pyrite grains, (c) typical sheetlike antimonite vein inside massive realgar antimonite partially corroded during hypergenesis, and (d) veins of hypidiomorphic pyrite corroded by allotriomorphic realgar.

and LOJ/3 are identical and contain micron inclusions along traces, areas of growth of quartz grains, or healed cracks (Figs. 10d, 10g). These samples also contain several fluid inclusions that, when heated, yielded limited results (Figs. 10c, 10e).

As a result of studies, it was found that homogenization temperatures T_{hom} of inclusions in the quartz of Sb–As veins in the Lojane deposit vary from 180 to 220°C, with $T_{hom} = 201°$ on average (Table 3; Fig.11).

RESULTS OF STUDYING SULFUR ISOTOPES

Five samples of antimonite and five samples of Realgar were selected for analysis of sulfur isotopes, thus complementing previous data (Mudrinic, 1978). The values of $\delta^{34}S$ for realgar averaged −1.61‰ with a range of 6.72‰, while the values averaged −1.92‰ with a range of 4.93‰ for the antimonite,. The distribution of the measured values of $\delta^{34}S$ is shown in Fig. 12.

Although our values of $\delta^{34}S$ in sulfides (from −5.19‰ to +1.19‰) are mostly negative, they are quite close to the isotopic sulfur composition of the mantle source. This is consistent with previous conclusions (Seal, 2006). Relatively recent studies have shown that negative values of $\delta^{34}S$ in hydrothermal ore sulfides are the result of the removal of H_2S in the gas phase during fluid boiling (Hagemann et al., 1994; Chodkiewicz et al., 2009).

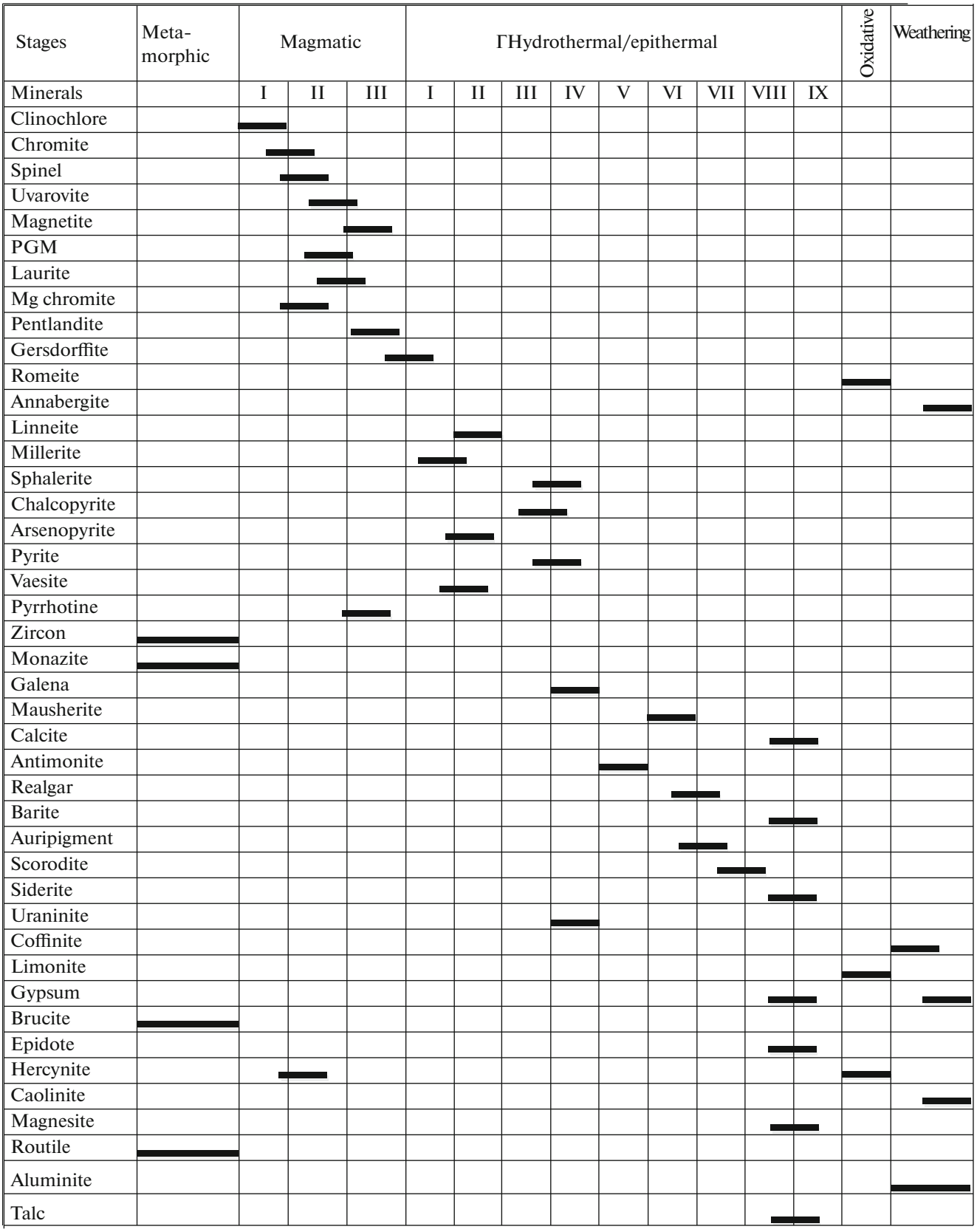

Fig. 7. Scheme of mineral formation sequence at the Lojane deposit. MPG—minerals of the platinum group.

Table 1. Content of main and related elements in ores of the Lojane deposit

Elements, g/t	Samples											
	LO1 EX48	LO1A EX48	LO2 EX48	LO2A EX48	LO3-Ant:	LO3A-Ant:	LO4	LO4A 22	LO5	LO5A	LO6 EX18	LO6A EX18
Ag	<0.5	1.2	0.8	1.01	1.15	<0.5	0.75	0.7	<0.5	1.8	<0.5	0.85
Al %	0.24	0.27	1.12	0.1	0.31	0.65	0.3	0.6	2.76	0.3	5.6	0.11
As %	4.90	5.10	1.45	6.39	0.64	5.35	0.95	0.59	0.22	6.92	0.80	4.92
Ba	<10	10	10	10	10	<10	<10	<10	10	10	10	<10
Be	0.85	1.12	0.8	0.7	<0.5	1.95	2	1.5	1.7	1.2	<0.5	0.6
Bi	1.2	1.56	1.13	1.85	2.7	0.95	1.8	2.3	2.15	0.98	1.56	2.2
Ca %	2.9	0.51	3.22	2.67	0.35	0.16	0.15	0.06	0.04	0.05	2.46	0.86
Cd	1.14	0.95	<0.5	1.53	1.2	0.88	1.35	1.12	0.65	<0.5	1.6	0.9
Co	65	86	32	6	11	53	32	50	41	43	51	50
Cr	1550	2160	1249	2070	5060	>10000	6040	3630	8950	>10000	1205	5273
Cu	7	87	4	4	68	6	4	64	75	7	7	7
Fe %	3.8	4.45	3.64	4.21	6.08	5.31	6.73	5.59	6.33	6.76	3.92	5.55
Ga	3.2	2.8	1.52	8.6	2.8	4.12	8.5	1.25	2.4	5.8	10.1	1.5
K %	0.09	0.07	0.04	0.02	0.02	0.01	0.01	0.04	0.01	0.01	0.06	1.35
La	8.2	12.1	13.2	6.7	17.1	7.2	9.5	21.1	8.8	11.4	8.2	8.8
Mg %	18.5	20.3	19.1	12	21.4	15	21.1	6.5	21.1	20.9	13.5	13.35
Mn	935	865	345	863	794	964	798	463	234	797	943	361
Mo	98	175	68	105	156	62	75	80	35	130	25	70
Na %	0.21	0.01	0.01	0.01	0.01	0.2	0.01	0.09	0.01	0.01	0.01	0.02
Ni	2023	1010	1020	1280	1200	124	53	36	744	465	435	1090
P	40	50	<10	50	<10	20	10	<10	30	20	90	50
Pb	1.2	1.32	1.25	5	2	2	2	2.15	1.85	2	1.5	1.4
S %	0.21	0.14	0.15	0.44	0.65	0.45	0.12	0.23	0.2	0.19	0.72	0.46
Sb %	2.32	5.17	1.54	2.99	4.03	1.84	1.49	1.42	0.77	3.75	0.36	1.46
Sc	17	64	4	5	8	7	5	4	5	77	4	4
Sr	34	56	8	8	99	6	4	3	3	6	8	47
Th	2.3	5.16	6.8	8.32	2.15	2.17	1.77	0.5	0.21	0.82	0.32	0.75
Ti %	<0.01	0.03	0.02	0.02	<0.01	0.01	0.01	0.09	0.02	0.02	0.08	0.06
Tl	58.46	32.88	32.56	18.24	33.95	33.37	132.7	188.2	127.5	44.37	56.3	45.2
U	19.5	23.9	23.1	4.6	5.3	10.4	10.2	34.9	22.2	10.8	44.2	10.9
V	54	23	19	17	43	54	36	87	4	34	23	6
W	3.5	1.9	5.2	2.4	1.55	12.5	15	12.5	50	1.4	80.2	7.8
Zn	54	76	67	65	32	19	54	20	52	43	23	56
U/Th	8.48	4.63	3.39	0.55	2.46	4.79	5.76	69.8	105.7	13.2	138.1	14.5
Co/Ni	0.03	0.08	0.03	0.01	0.01	0.43	0.6	1.38	0.05	0.09	0.01	0.04

Concentrations of Al, Mg, Ti, K, Na, S, As, and Sb are given in wt %. Concentrations of other elements are given in g/t.

Table 2. Content of main and related elements in ore concentrates, enrichment tails, and host rocks (serpentinites) of the Lojane deposit

Elements, g/t	Samples						
	Flotation tails			Serpentinites	Ore concentrates		
	LO-1/1	LO-1/2	LO-1/3	LO-1/4	LO-3/1	LO-3/2	LO-3/3
Ag	0.13	0.11	0.13	0.10	0.12	0.20	0.08
Al %	1.43	2.77	3.74	4.47	0.25	1.02	0.19
As	9987	5619.2	3226	1017	25000	35200	24500
Ba	100	243	348	330	45	51	48
Be	1	3	2	2	1	1	1
Bi	0.33	0.31	0.36	0.67	0.17	0.3	0.18
Ca %	5.02	6.58	6.23	4.87	1.46	2.12	0.99
Cd	0.29	0.23	0.14	0.27	0.71	0.68	0.47
Ce	11.36	26.09	33.25	46.43	1.5	4.61	1.89
Co	109.6	74.9	87.5	56.9	12.1	18.8	54.1
Cr	3276	2927	1476	3019	131	316	74
Cs	16.5	17.9	23.7	4.6	7.3	9.2	4.3
Cu	22.7	42.9	106.8	33.2	3.3	5.6	9.1
Dy	1.1	2	2.3	2.9	0.2	0.4	0.2
Er	0.7	1.1	1.5	1.4	0.1	0.3	0.1
Eu	0.2	0.3	0.5	0.9	0.1	0.1	0.1
Fe	4.77	3.45	3.06	4.06	1.32	1.75	1.25
Ga	3.78	7.31	8.74	10.57	0.65	2.5	0.69
Gd	1.3	2.1	2.6	3.3	0.1	0.4	0.1
HF	0.58	1.08	1.83	1.5	0.02	0.02	0.02
Ho	0.3	0.5	0.5	0.6	0.1	0.1	0.1
In	0.03	0.02	0.02	0.01	0.02	0.01	0.02
K %	0.35	1.1	1.21	1.47	0.07	0.35	0.05
La	4	11.8	15.2	23.9	0.1	1.6	0.2
Li	31.2	31.8	35.7	22.9	3.8	7.2	4.1
Lu	0.1	0.2	0.2	0.2	0.1	0.1	0.1
Mg %	6.39	4.98	4.12	5.71	0.1	0.33	0.13
Mn	963	949	878	726	10	32	22
Mo	52.61	19.99	22.79	16.54	171.65	152.86	123.76
Na %	0.18	0.42	0.55	0.54	0.03	0.14	0.05
Nb	1.78	4.01	5.32	8.11	0.04	0.04	0.04
Nd	5	11.8	15.7	19.2	0.4	1.9	0.8
Ni	1917.8	939.5	1674.8	1125.5	207.2	364.6	914.9
P	0.01	0.02	0.03	0.13	0.01	0.01	0.01
Pb	286.82	55.91	25.64	30.3	1.38	8.24	7.18
Pr	1.3	3.2	4.1	5.6	0.1	0.5	0.2
Rb	22.6	60.8	74.1	75.2	4.2	18.8	2.3
Re	0.01	0.01	0.01	0.01	0.01	0.01	0.03
S %	1.41	0.62	0.68	0.27	10	7.85	10
Sb	10000	10000	10000	553.69	10000	10000	10000
Sc	7.6	8.5	7.5	9.7	0.1	0.2	0.3

Table 2. (Contd.)

Elements, g/t	Samples						
	Flotation tails			Serpentinites	Ore concentrates		
	LO-1/1	LO-1/2	LO-1/3	LO-1/4	LO-3/1	LO-3/2	LO-3/3
Se	1.2	0.6	0.9	1.2	0.4	0.3	0.8
Sm	1.2	2.6	2.9	4.2	0.2	0.4	0.2
Sn	1.3	1.7	2.4	1.9	0.6	1.1	0.5
Sr	129	181	174	90	13	35	18
Ta	0.2	0.4	0.5	0.7	0.1	0.1	0.1
Tb	0.1	0.3	0.4	0.5	0.1	0.1	0.1
Te	1.41	1.24	0.97	0.95	0.05	0.05	0.05
Th	2.6	5.6	7.5	8.8	0.1	0.1	0.1
Ti	470	1010	1290	1950	10	10	10
Tl	53.87	31.5	34.38	1.01	177.22	205.78	129.85
Tm	0.1	0.2	0.2	0.3	0.1	0.1	0.1
U	21.1	25.3	27.8	4.3	28.8	21	10.6
V	39	40	40	64	3	10	2
W	80.2	69.9	64.2	3.4	1.9	4.1	5.5
Y	7.3	12.1	13.5	15.1	0.8	2.4	1
Yb	0.6	1	1.2	1.6	0.1	0.3	0.1
Zn	73.8	52.7	40.6	94.2	16.5	20.6	49.6
Zr	16.8	39.1	52.3	51.6	0.2	0.2	0.3
∑REE	27.36	63.19	80.55	111.03	3.30	10.91	4.29
∑LREE	23.06	55.79	71.65	100.23	2.40	9.11	3.39
∑HREE	4.30	7.40	8.90	10.80	0.90	1.80	0.90
Hf/Sm	0.48	0.41	0.63	0.36	0.10	0.05	0.10
Nb/La	0.44	0.34	0.35	0.34	0.40	0.02	0.20
Th/La	0.65	0.47	0.49	0.37	1.00	0.06	0.50
Y/Ho	24.33	24.20	27.00	25.17	8.00	24.00	10.00
U/Th	8.11	4.52	3.71	0.49	288.00	210.00	106.00
Rb/Sr	0.17	0.34	0.43	0.84	0.32	0.54	0.13
Co/Ni	0.06	0.08	0.05	0.05	0.06	0.05	0.06
Te/Se	1.17	2.07	1.08	0.79	0.12	0.17	0.06
Eu/Eu*	0.74	0.52	0.67	0.82	1.07	0.76	1.07
Ce/Ce*	1.33	1.09	1.10	0.99	3.34	1.39	3.04
∑Ce	21.66	52.89	68.25	95.13	2.10	8.61	3.09
∑Y	4.20	7.80	9.20	12.40	0.80	1.50	0.80
∑Sc	1.50	2.50	3.10	3.50	0.40	0.80	0.40
Eu/Sm	0.17	0.12	0.17	0.21	0.50	0.25	0.50

Concentrations of Al, Mg, Ti, K, Na, and S are given in wt %. Concentrations of trace elements are given in g/t. ICP-MS analyses were performed at BVM. $EU/EU^* = EU_N/((EU_N)1/2)1/2)$; $CE/CE^* = CE_N/((2LA_N + SM_N)/3)$; REE—REE; LREE—light REE; HRE—heavy REE.

Table 3. Homogenization temperatures T_{hom} of biphasic liquid inclusions in quartz (samples LOJ/2 and LOJ/3)

	LOJ/2 (1)	LOJ/2 (2)	LOJ/2 (3)	LOJ/2 (4)	LOJ/3 (1)	LOJ/3 (2)	LOJ/3 (3)	LOJ/3 (4)	LOJ/2 (5)	Max.	Min.	Medium
T_{hom}	186	201	181	182	211	195	219	217	215	219	181	201

(1) is the inclusion number in order.

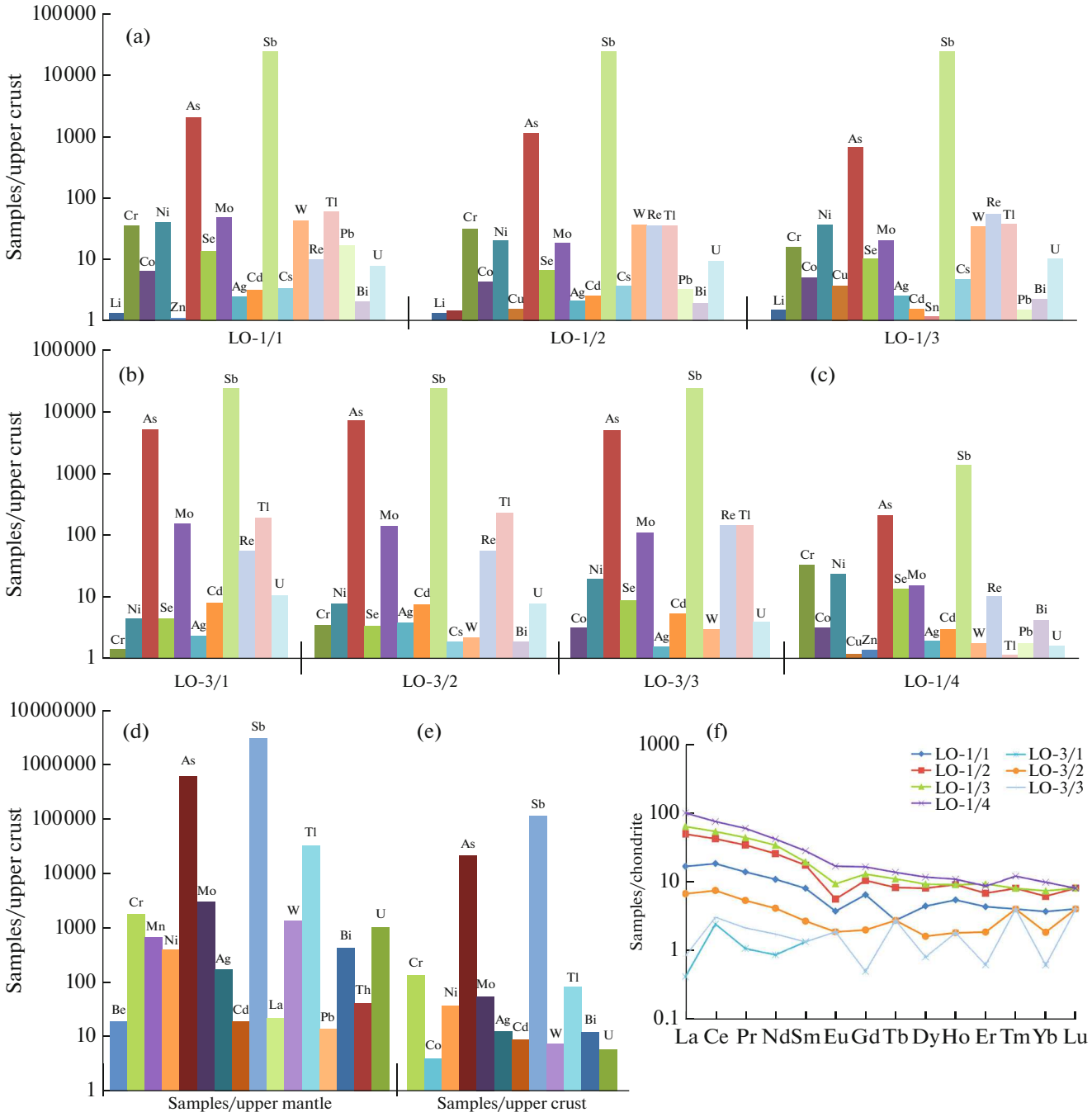

Fig. 8. Distribution of (a–e) major trace elements and (f) REE in (a) tailings, (b) concentrate, and (c) host rocks and epithermal ores; (d, e) mean values of the Logan deposit normalized to the average for the (a–c, e) upper crust and (d) upper mantle (Taylor and McLennan, 1988); and (f) REE normalized to chondrite (McDonough and Sun, 1995). Samples LO-1/1–LO3/3—samples (see Table 2). (d, e) Are the average values for ore samples (see Table 1).

CONCLUSIONS

The main features of the Lojane deposit are as follows that ore mineralization is represented by antimonite and realgar subordinate to orpiment and localized in the form of quartz veins and veins of feather morphology, mainly localized in contact between rhyolites and serpentinites.

Five types of Sb–As ores were identified in the Lojane deposit: brecciated realgar orpiment ores; realgar breccias; brecciated antimonite ores; massive, almost monomineral realgar ores; and realgar–antimonite nest-shaped ores. Ores are characterized not only by the unusual paragenesis of minerals of nickel, arsenic, and antimony, but also by a very close fusion

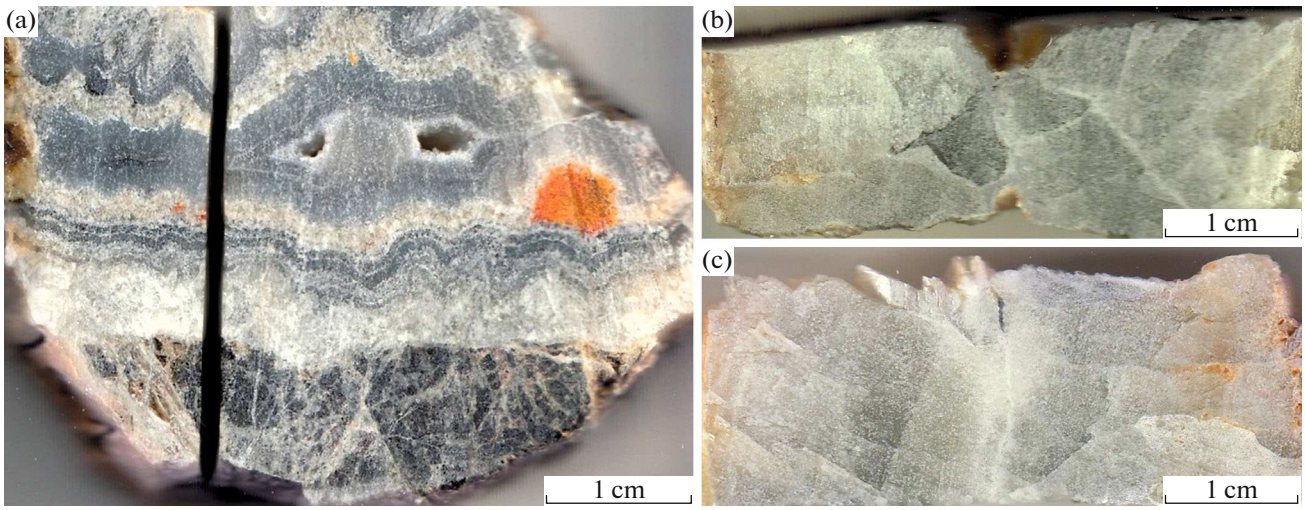

Fig. 9. Samples of quartz from epithermal Sb–As ores of the Lojane deposit. (a) Collomorphic-striped quartz vein with realgar (orange); (b, c) pale green quartz from epithermal veins.

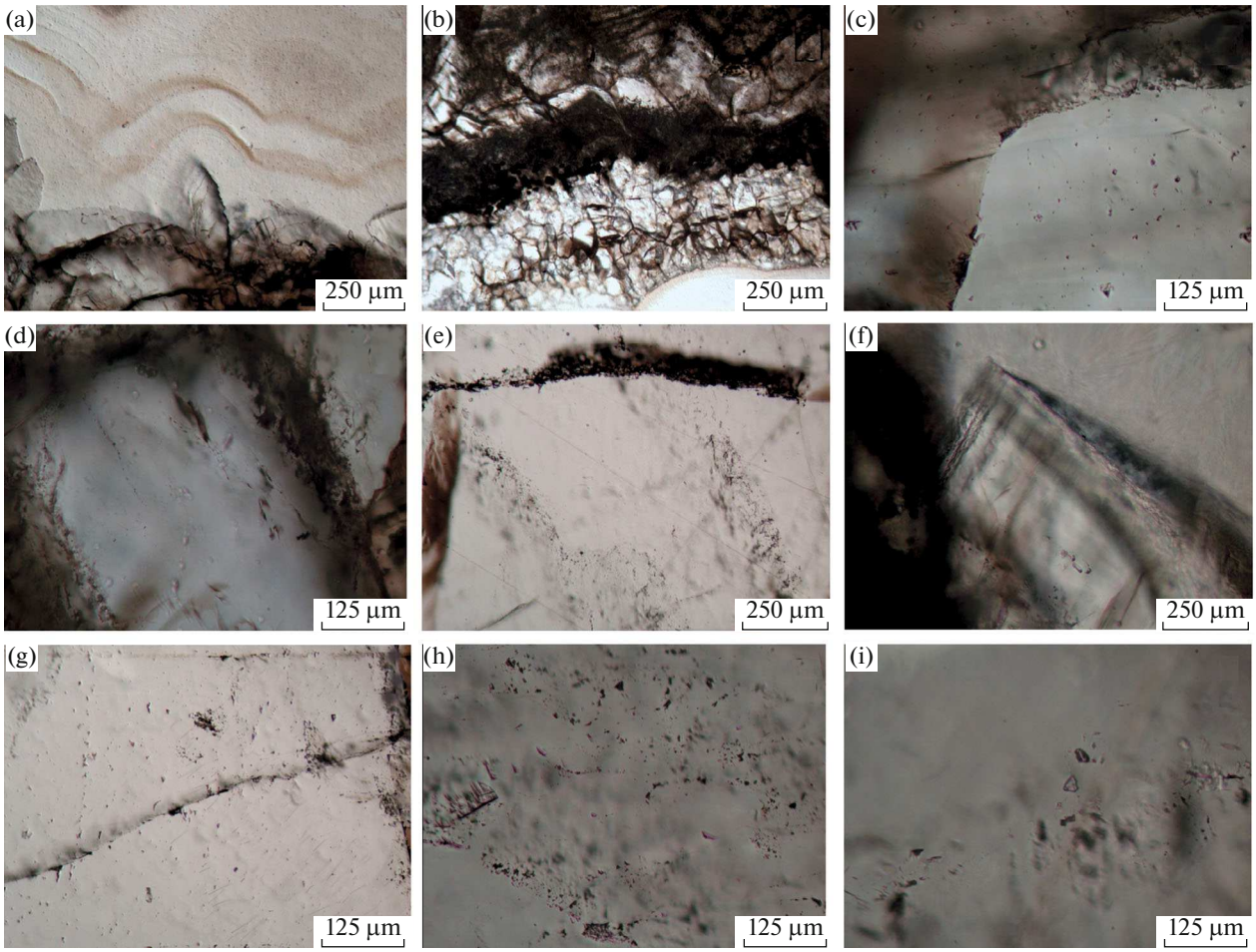

Fig. 10. Microphotographs of bilaterally polished quartz plates from epithermal Sb–As veins of the Lojane deposit. (a) Collomorphic microgranular quartz free from fluid inclusions, sample LOJ/1; (b) coarse-grained quartz alternating with collomorphic quartz, sample LOJ/1; (c) very small fluid inclusions, in which it is difficult to detect phases, sample LOJ/1. (d) fluid inclusions modified after capture and therefore empty, sample LOJ/1; (e, f) micronic inclusions along the traces of either growth zones or healed fractures, (e) sample LOJ/2, (f) sample LOJ/3; (g, h) micronic inclusions along the traces of either growth zones or healed fractures, (g) sample LOJ/2, (h) sample LOJ/3; (i, j) two-phase fluid inclusions in quartz, (i) sample LOJ/2, (j) two-phase fluid inclusions in quartz, sample LOJ/3; and (k) fluid inclusions modified after capture and therefore empty, sample LOJ/3. Flat-polarized light.

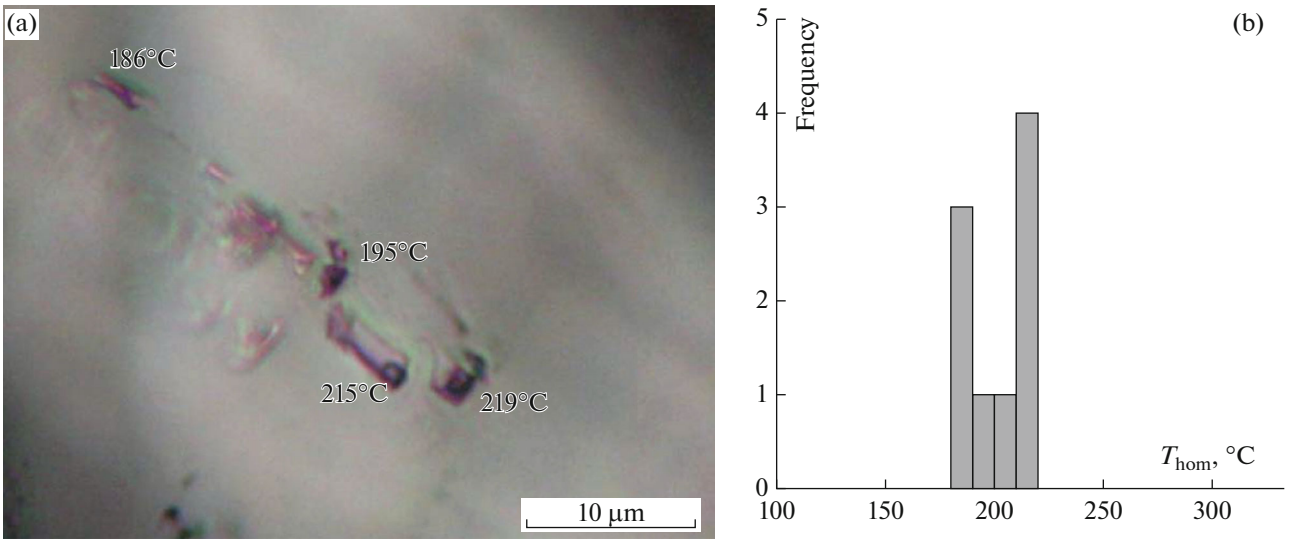

Fig. 11. (a) Photograph of biphasic fluidic inclusions in quartz with corresponding homogenization temperature, sample LOJ/3; (b) histogram of homogenization temperature distribution, samples LOJ/2 and LOJ/3.

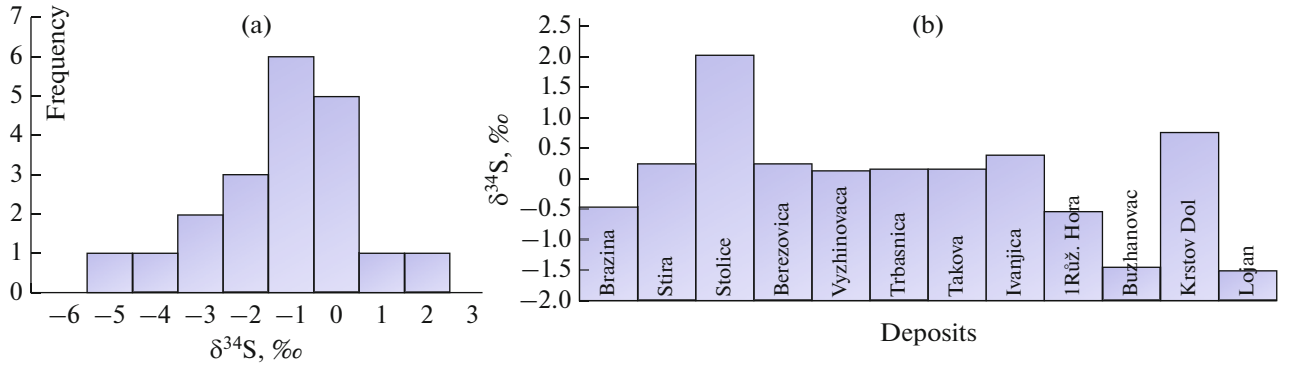

Fig. 12. (a) Histogram of the isotopic composition of sulfur in the sulfides of the Lojane deposit and (b) the value of δ^{34}S in the deposits of the Serbo-Macedonian metallogenic province according to (Mudrinic, 1978).

of antimonite, realgar, collomorphic quartz, and silica.

The enrichment of the Lojane deposit ores with a wide range of trace elements (Sb, As, Cr, Ni, Se, Mo, Re, Bi, Co, Cd, Ag, W, Cu, Pb, Zn, Tl, and U), compared to the average values of the upper crust. This spectrum range appears to be due to the combination of several different time paragenesis in mineralization ores. Increased concentrations of Ni, Co, Cr in Sb–As ores of the Lojane deposit clearly indicate their mobilization from host ultrabasic rocks. As we noted earlier, the spectrum of enrichment with trace elements of host serpentinites (Fig. 8b) is not less wide than that of the ore, tails, and concentrates (Figs. 8a, 8b, 8e); however, the enrichment factors are an order of magnitude or more lower. It is likely that the host serpentinites can serve as a source of not only increased contents of Ni, Co, Cr, and Tl, but also the main (Sb, As) ore components.

With increasing pressure, light REE pass into an aqueous fluid, and heavy ones are retained in magma, which allows the first to be considered "hydrophilic" elements and the second "magmaphilic" elements (Zharikov et al., 1999). The data in Table 2 and Fig. 8e show that, in the studied ores and the serpentenites containing them, the "hydrophilic" REE of the "cerium" group predominate. Graphs normalized to chondrite REE for serpentinites form a slightly inclined twin-chondrite spectrum with a small europium minimum (see Fig. 8e).

According to a small number of measurements of homogenization temperature T_{hom}, inclusions in quartz ranged from 180 to 220°C—on average, 201°C (Table 3; Fig. 11). This temperature range corresponds to the epithermal conditions of deposition of As- and Sb-sulfides (Munoz and Shepherd, 1987; Ferrini et al., 2003) and to the temperatures established for similar

deposits in Greece, Turkey, etc. (Ozgur et al., 1997; Voudouris et al., 2008).

The isotopic composition of sulfur in the antimonite and realgar of the Lojane deposit, as well as other deposits of the Serbo-Macedonian metallogenic province (Fig. 12b), indicates its endogenous origin. As we noted earlier, Lojane samples contained a fusion of antimonite, realgar, and pyrite, but the overall absence of sulfates probably indicates relatively low conditions of fO_2, which is consistent with work (Ohmoto, 1972), which showed H_2S to most likely dominate in fluids. Numerous previous studies of similar deposits in other regions of the world have shown H_2S to dominate ore-forming fluid, while temperature had little effect on the isotopic composition of its sulfur (Ohmoto and Rye, 1979).

The presence of barite in the later stages of mineralization of the Lojane deposit indicates a certain increase in oxygen volatility, which may have contributed to the fractionation of sulfur isotopes with the removal of isotopic-light sulfur in the crystallization of sulfate with isotopic-heavy sulfur (Ohmoto, 1972; Mudrinis, 1978; Kesler et al., 1981; Volkov et al., 2006; Strmiz, Palinkas, 2018).

The epithermal nature of Sb–As mineralization of the Lojane deposit is determined by the textured features of the ores, the temperature conditions of mineral formation, and the spatial distribution of mineralization, as well as mineralogical and geochemical features.

ACKNOWLEDGMENTS

The authors express their special gratitude to Prof. Vasilos Melfos of Aristotle University of Thessaloniki, Greece, for his assistance in the study of fluid inclusions in the Lojane quartz deposit. At the same time, we are sincerely grateful to Kaltun Madencilik, Skopje, which provided us with the opportunity to visit the Lojane deposit and select the necessary collection of samples.

FUNDING

This article was prepared within the framework of the topic of a state order to the Institute of Geology of Ore Deposits, Petrography, Mineralogy, and Geochemistry, Russian Academy of Sciences.

CONFLICT OF INTEREST

The authors declare that they have no conflicts of interest.

REFERENCES

Alderton, D., Serafimovski, T., Burns, L., and Tasev, G., Distribution and mobility of arsenic and antimony at mine sites in FYR Macedonia, *Carpathian J. Earth Environ. Sci.*, 2014, vol. 9, no. 1, pp. 43–56.

Antonovic, A., *Geology, Tectonic Structure and Genesis of the Arsenic-Antimony Ore Deposits in Tzome Lojane and Nikustak district (Skopska Crna Gora Mts)*, Skopje: Geol. Inst., 1965, Spec. Iss. 1 (in Serbian).

Augé, T., Morin, G., Bailly, L., and Serafimovski, T., Platinum-group minerals and the host chromitites in Macedonian ophiolites, *European J. Mineral.*, 2017, vol. 29, pp. 585–596.

Bau, M., Rare-earth element mobility during hydrothermal and metamorphic fluid-rock interaction and the significance of the oxidation state of europium, *Chem. Geol.*, 1991, vol. 93, pp. 219–230.

Boev, B. and Jankovic, S., Nickel and nickelferous iron deposits of the Vardar Zone (SE Europe) with particular reference to the Rzanovo-Studena Voda ore-bearing series, in *Faculty of Mining and Geologytip, St. Cyril and Methodius University*, 1996, Spec. Iss. 3, pp. 270–278.

Bortnikov, N.S., Gamyanin, G.N., Vikent'eva, O.V., Prokof'ev, V.Yu., Alpatov, V.A., and Bakharev, A.G., Fluid composition and origin in the hydrothermal system of the Nezhdaninsky Gold Deposit, Sakha (Yakutia), Russia, *Geol. Ore Deposits*, 2007, vol. 49, no. 2, pp. 87–128.

Deleon, G., *Structural characteristics of arsenic-antimony ore from the Lojane mine, Glasnik Prirod. Muzeja u Beogradu*, 1959, Ser. A, vol. 11, pp. 109–114 [in Serbian].

Djordjevic, T., Kolitsch, U., Serafimovski, T., Tasev, G., Tepe, N., Stoger-Pollach, M., Hofmann, T., and Boev, B., Mineralogy and weathering of realgar-rich tailings at a former As-Sb-Cr mine at Lojane, North Macedonia, *Can. Mineral.*, 2019, vol. 57, pp. 1–21.

Ferrini, V., Martarelli, L., De Vito, C., Cina, A., and Deda, T., The Koman dawsonite and realgar-orpiment deposit, Northern Albania: Inferences on processes of formation, *Can. Mineral.*, 2003, vol. 41, pp. 413–427.

Goryachev, N.A., Vikent'eva, O.V., Bortnikov, N.S., Prokof'ev, V.Yu., Alpatov, V.A., and Golub, V.V., The world-class Natalka gold deposit, northeast Russia: REE patterns, fluid inclusions, stable oxygen isotopes, and formation conditions of ore, *Geol. Ore Deposits*, 2008, vol. 50, no. 5, pp. 362–390.

Grafenauer, S., Genesis of chromite in Yugoslavian peridotite, in *Time- and Strata-Bound Ore Deposits*, Klemm, D.D. and Schneider, H.-J., Eds., Verlag-Berlin–Heidelburg: Springer, 1977, pp. 327–351.

Hagemann, S.G., Gebre-Mariam, M., and Groves, D.I., Surface-water influx in shallow-level Archean lode-gold deposits in Western Australia, *Geology*, 1994, vol. 22, pp. 1067–1070.

Hiessleitner, G., Geologie mazedonischer Chromeisenlagerstäatten. Berg- und Hüttenmännisches *Jahrb. Montan. Hochsch. Leoben*. 1931, vol. 179, pp. 47–57 [in German].

Hiessleitner, G., Einbruch von Granit und Andesit in Chromerze führenden Serpentin von Lojane, NNW Kumanovo in Südserbie, *Z. Prakt. Geol.*, 1934, vol. 42, pp. 81–88 [in German].

Hiessleitner, G., Serpentin- und Chromerz-Geologie der Balkanhalbinsel und eines Teiles von Kleinasien, *Jahrb.*

Geol. Bundesanst. Sonderb., 1951, vol. 1, pp. 1–255 [in German].

Hodkiewicz, P.F., Groves, D.I., Davidson, G.J., Weinberg, R.F., and Hagemann, S.G., Influence of structural setting on sulphur isotopes in Archean orogenic gold deposits, Eastern Goldfields Province, Yilgarn, Western Australia, *Miner. Depos.*, 2009, vol. 44, pp. 129–150.

Jankovic, S., General characteristics of the antimony ore deposits of Yugoslavia, *Neues Jahrb. Mineral., Abh.*, 1960, vol. 94, pp. 506–538 [in German].

Jones, B. and Manning, D.A.C., Comparison of geochemical indices used for the interpretation of palaeoredox conditions in ancient mudstones, *Chem. Geol.*, 1994, vol. 111, pp. 111–129.

Kesler, E.S., Ewing, R., Deditius, A., Reich, M.M., Utsunomiya, S., and Chryssoulis, S., Role of arsenian pyrite in hydrothermal ore deposits: A history and update, in *Proc. 6th Geol. Soc. Nevada on Great Basin Evolution and Metallogeny*, Lancaster, DEStech Publ., 2010, pp. 233–245.

Kolitsch U., Dordevic, T., Tasev, G., Serafimovski, T., Boev, I., and Boev, B., Supergene mineralogy of the Lojane Sb—As–Cr deposit, Republic of Macedonia: Tracing the mobilization of toxic metals, *Geol. Macedonica*, 2018, vol. 32, no. 2, pp. 95–117.

Kun, L., Ruidong, Y., and Wenyong, Ch., Trace element and REE geochemistry of the Zhewang gold deposit, southeastern Guizhou Province, China, *Chinese J. Geochem.*, 2014, vol. 33, pp. 109–118.

Manning, D.A.C., Comparison of geochemical indices used for the interpretation of palaeoredox conditions in ancient mudstones, *Chem. Geol.*, 1994, vol. 111, pp. 111–129.

McDonough, W.F. and Sun, S.S., The composition of the Earth, *Chem. Geol.*, 1995, vol. 120, pp. 223–253.

Mineev D.A., *Lantanoidy v rudakh redkozemel'nykh i kompleksnykh mestorozhdenii* (Lanthanoids in the Ores of Complex and Rare-Earth Fields), Moscow: Nauka, 1974 [in Russian].

Monecke, T., Kempe, U., and Gotze, J., Genetic significance of the trace element content in metamorphic and hydrothermal quartz: A reconnaissance study, *Earth Planet. Sci. Lett.*, 2002, vol. 202, pp. 709–724.

Mudrinic, C., *Geochemical Features of Sb-As Associations in the Serbo-Macedonian metallogenic province, PhD Thesis*, Faculty of Mining and Geology, Belgrade, 1978 [in Serbian].

Munoz, M. and Shepherd, T.J., Fluid inclusion study of the Bournac polymetallic (Sb-As-Pb-Zn-Fe-Cu...) vein deposit (Montagne Noire, France), *Miner. Depos.*, 1987, vol. 22, pp. 11–17.

Ohmoto, H., Systematics of sulfur and carbon isotopes in hydrothermal ore deposits, *Econ. Geol.*, 1972, vol. 67, pp. 551–578.

Ohmoto, H. and Rye, R.O., *Isotopes of sulfur and carbon, Geochemistry of Hydrothermal Ore Deposits*, 2nd ed., Barnes, H.L., Ed., New York: Wiley, 1979, pp. 509–567.

Oreskes, N. and Einaudi, M.T., Origin of rare-earth element enriched hematite breccias at the Olympic Dam Cu–U–Au–Ag deposit, Roxby Downs, South Australia, *Econ. Geol.*, 1990, vol. 85, no. 1, pp. 1–28.

Ozgur, N., Halbach, P., Pekdeger, A., Sommer-von Jarmersted, C., Sonmez, N., Dora, O.O., Ma, D.S., Wolf, M., and Stichler, W., Epithermal antimony, mercury and gold deposits in the rift zone of the Küçük Menderes, Western Anatolia, Turkey: preliminary studies, in *Mineral Deposits, Research and Exploration (Where do they meet?), Proc. 4th Biennial SGA Meet., Turku, Finland, August, 1997*, pp. 269–272.

Pamic, J., Tomljenovic, B., and Balen, D., Geodynamic and petrogenetic evolution of Alpine ophiolites from the central and NW Dinarides: an overview, *Lithos*, 2002, vol. 65, pp. 113–142.

Pokrovski, G.S., Zakirov, I.V., Roux, J., Testemale, D., Hazemann, J., Bychkov, A.Y., and Golikova, G.V., Experimental study of arsenic speciation in vapor phase to 500°C: Implications for as transport and fractionation in low-density crustal fluids and volcanic gases, *Geochim. Cosmochim. Acta*, 2002, vol. 66, pp. 3453–3480.

Radusinovic, D.R., Greigite from the Lojane chromium deposit, Macedonia, *Am. Mineral.*, 1966, vol. 51, pp. 209–215.

Robertson, A.H.F., Overview of the genesis and emplacement of Mesozoic ophiolites in the Eastern Mediterranean Tethyan region, *Lithos*, 2002, vol. 65, pp. 1–67.

Saravanan, C.S. and Mishra, B., Uniformity in sulfur isotope composition in the orogenic gold deposits from the Dharwar Craton, Southern India, *Miner. Deposita*, 2009, vol. 44, pp. 597–605.

Schmid, S.M., Bernoulli, D., Fugenschuh, B., Matenco, L., Schefer, S., Schuster, R., Tischler, M., and Ustaszewski, K., The Alpine–Carpathian-Dinaridic orogenic system: correlation and evolution of tectonic units, *Swiss J. Geosci.*, 2008, vol. 101, pp. 139–183.

Schumacher, F., The ore deposits of Yugoslavia and the development of its mining industry, *Econ. Geol.*, 1954, vol. 49, pp. 451–492.

Seal, R.R., Sulfur isotope geochemistry of sulfide minerals, *Rev. Mineral. Geochem.*, 2006, vol. 61, pp. 633–677.

Serafimovski, T., *Structural-Metallogenic Features of the Lece-Chalkidiki Zone: Types of Mineral Deposit and Distribution*, Stip: Faculty of Mining, 1993, Spec. Iss. 2.

Serafimovski, T. and Tasev, G., Sulfur isotope compositions from different type of deposits in the Buchim-Damjan-Borov Dol ore district, Eastern Macedonia, in *Proc. 10th Appl. Isotope Geochem. Conf., Hungarian Acad. Sci., September 22–27, 2013, Budapest, Hungary*, 2013, pp. 8–13.

Strmic Palinkas, S., Hofstra, H.A., Percival, J.T., Borojevic Sostaric, S., Palinkas, L., Bermanec, V., Pecskay, Z., and Boev, B., Comparison of the Allchar Au–As—Sb–Tl Deposit, Republic of Macedonia, with Carlin-Type Gold Deposits, Chapter 10, *Rev. Econ. Geol.*, 2018, vol. 20, pp. 335–363.

Tasev, G., Serafimovski, T., Djordjevic, T., and Boev, B., Soil and groundwater contamination around Trоме Lojane As-Sb mine, Republic of Macedonia, in *Proc. 17th Int. Mul-*

tidisciplinary Sci. GeoConf. SGEM, 2017, vol. 17, pp. 809–817.

Tasev, G., Serafimovski, T., Boev, B., and Gjorgjiev, L., Morphological types of mineralization in the Lojane As–Sb deposit, Republic of Macedonia, in *Proc. 18th Int. Multidisciplinary Sci. GeoConf. SGEM*, 2018, vol. 13, pp. 601–608.

Taylor, S.R. and McLennan, S.M., *Continental Crust: Its Composition and Evolution*, Oxford: Blackwell Sci., 1985.

Tzamos, E., Gamaletsos, N.P., Grieco, G., Bussolesi, M., Xenidis, A., Zouboulis, A., Dimitriadis, D., Pontikes, Y., and Godelitsas, A., New insights into the mineralogy and geochemistry of Sb ores from Greece, *Minerals*, 2020, vol. 10, pp. 1–16.
https://doi.org/10.3390/min10030236

Volkov, A.V., Serafimovskii, T., Kochneva, N.T., Tomson, I.N., and Tasev, G., The Alshar epithermal Au-As-Sb-Tl deposit, southern Macedonia, *Geol. Ore Deposits,* 2006, vol. 48, no. 3, pp. 175–192.

Voudouris, P., Melfos, V., Spry, P.G., Bonsall, T., Tarkian, M., and Economou-Eliopoulos, M., Mineralogical and fluid inclusion constraints on the evolution of the Plaka intrusion-related ore system, Lavrion, Greece, *Mineral. Petrol.*, 2008, vol. 93, pp. 79–110.

Zharikov, V.A., Gorbachev, N.S., Lightfoot, P., and Doherti, W., Rare earth element and yttrium distribution between fluid and basaltic melt at pressures of 1-12 kbar: Evidence from experimental data, *Dokl. Ross. Akad. Nauk*, 1999, vol. 366, no. 2, pp. 239–241.

Zotov, A.V., Shikina, N.D., and Akinfeev, N.N., Thermodynamic properties of the Sb(III) hydroxide complex $Sb(OH)_3(aq)$ at hydrothermal conditions, *Geochim. Cosmochim. Acta*, 2003, vol. 67, pp. 1821–1836.